

Design Analysis of Mid IR DIAL System for Detection of Hazardous Chemical Species

M.K. Jindal[#], Mainuddin^{§,*}, S. Veerabuthiran¹ and Atul Kumar[#]

[#]DRDO-Instruments Research & Development Establishment, Dehradun - 248 008, India

[§]Department of Electronics & Communication Engineering, Jamia Millia Islamia, Delhi - 110 025, India

¹DRDO-Centre for High Energy Systems and Sciences, Hyderabad - 500 053, India

*E-mail: mainuddin@jmi.ac.in

ABSTRACT

Nowadays, both military and public agencies are concerned with the remote detection of toxic gases and chemical warfare agents in the atmosphere. A promising method for the remote detection of such harmful chemicals in the atmosphere is Differential Absorption Lidar (DIAL). In the current paper, system design analysis has been carried out to build a DIAL system for the detection of toxic chemical warfare agents, chemical warfare simulants, explosive precursors, and pollutants. The proposed DIAL system comprises an Optical Parametric Oscillator (OPO) based tuneable laser, a 203 mm diameter Cassegrain telescope, a TE-cooled MCT detector, suitable data acquisition hardware, etc. The DIAL output parameters like return signals, SNR, and minimum measurable concentrations have been simulated under different weather conditions such as clear sky, moderately hazy sky, and hazy atmospheric conditions for given system input parameters (pulse energy, detectivity, bandwidth, DAQ resolution, etc.). We have considered chemicals such as Sarin, Thiodiglycol (TDG), acetone, and methane to be detected using the system. Analysis has been carried out for these chemicals present at different locations with varying concentrations. Our analysis reveals that the DIAL system with a laser transmitter of 5 mJ energy and 203 mm receiver telescope is capable of detecting a few ppm concentrations of toxic chemicals present anywhere between the ranges from a few tens of meters to 2 km with topographic target present. The sensitivity of the system in terms of minimum detectable concentrations for the considered chemicals is also estimated for different atmospheric conditions. It is seen that the minimum detectable concentration of TDG is 3.2 ppm in clear weather conditions which increases to 9.2 ppm under a hazy atmosphere. A similar analysis has been carried out for other toxic chemicals and has been discussed in the paper.

Keywords: LIDAR; DIAL; OPO; Toxic chemicals; Concentration

1. INTRODUCTION

In today's world, industrialization and weaponization have made a deep impact on the quality and health of the environment. Industrial discharge into the air, fossil fuel combustion in vehicles and factories, burning of carbon compounds, airplane propellants, chemical warfare, explosive chemicals, etc are among numerous reasons for atmospheric pollution. This poses serious health issues and life threats to human beings. Detection and identification of toxic chemicals and polluting agents are necessary for taking remedial action for a sustainable environment. There are various techniques reportedly used for the detection of chemical warfare agents¹⁻². Numerous detection methods have been employed, including ion mobility spectrometry, infrared spectrometry, Raman spectrometry, Fourier Transform Infrared (FTIR) spectroscopy, etc. The majority of methods used, for instance, to monitor dangerous compounds involve point sampling, which necessitates placing the sensor in a contaminated area. On the other hand, remote sensing techniques are an absolute

necessity for the fast detection of such chemical releases from safe standoff distances.

Within lidar also, there are different techniques based on the type of scattering and absorption phenomena. Specifically, Differential Absorption Lidar (DIAL) is the technique that is used for the detection and identification of toxic chemicals from standoff distances. DIAL also quantifies the concentration of the toxic chemical agent. This is done by calculating the ratio of the amplitude of return signals at two wavelengths, namely λ_{on} (lambda on) and λ_{off} (lambda off). The wavelength at which the target chemical agent has strong absorption is called λ_{on} or online wavelength. The wavelength at which the target agent has less absorption (as compared to online wavelength) is called λ_{off} or offline wavelength. The values of λ_{on} and λ_{off} are different for different toxic compounds. The DIAL is a flexible method and can be used to remotely detect many different chemicals. By taking advantage of concepts like atmospheric scattering and absorption, the DIAL method may provide spatially resolved measurements of these agents with adequate sensitivity (at a few ppm levels) at distances of several kilometers. Due to their long-range detection capability, sensitivity, and selectivity,

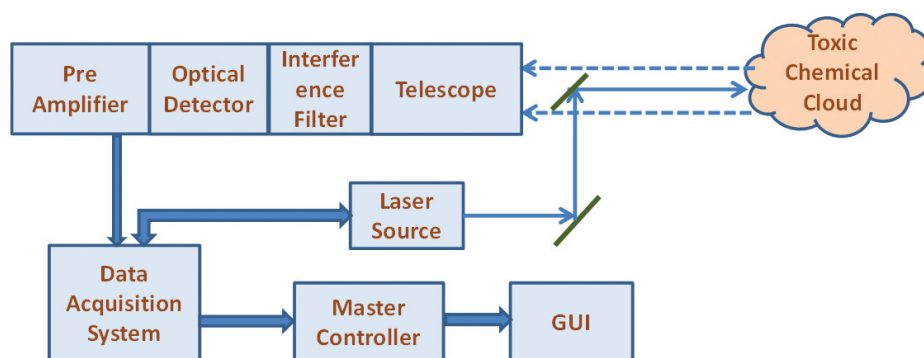


Figure 1. Block diagram of differential absorption lidar system.

systems based on DIAL technology are regarded as superior for the detection of chemicals.

As it corresponds with fundamental carbon-hydrogen stretch absorption, several chemical warfare agents and other toxic chemicals absorb light radiations in the mid-IR region³. Therefore, to detect these toxic chemicals using the DIAL system the laser transmitter should have wavelengths in this IR band. Specifically, the detection can be done in two wavelength bands within the IR band i.e., 2-5 μm wavelength band and 9-11 μm band⁴⁻⁵. The required energy levels in this wavelength slot are available in usually CO_2 laser (9-11 μm) and OPO laser (2-5 μm). Many research groups reported having used CO_2 lasers for the detection of hazardous chemicals⁶⁻¹¹. Some other researchers have used OPO lasers in a 2-5 μm band for the detection of hazardous chemicals in the atmosphere¹²⁻¹⁵. Choosing the particular wavelength band for DIAL applications involves many considerations like absorption characteristics of target chemical species, atmospheric propagation characteristics of laser, maintainability, and size of the laser, availability of detectors, availability of the number of wavelengths, etc.

For the current studies, we have selected a tunable OPO laser operating in a 3.0-3.45-micron wavelength band because of the reasons that it is a compact laser based on solid-state laser technology, has easier maintenance aspects, can give 450 different wavelength lines to cater to chemicals with sharp absorption spectrum, having almost constant energy at all the wavelengths and has lesser absorption by water molecules during atmospheric transmission. Many authors have reported their studies on the effects of atmospheric modelling and uncertainty analysis for sensors for gas absorption studies. The work reported by the authors.

Bril¹⁶, *et al.* is mainly focussed on the effect of errors in atmospheric modelling that introduces uncertainty in system output parameters, mainly aimed at the different wavelength bands (9 to 11 μm and 4.6 to 5.6 μm) and gives a solution to select the optimum laser wavelengths for minimum error in measurement due to interfering molecules. The work reported by Payne¹⁷, *et al.*, describes the errors in atmospheric models. Puiu¹⁸, *et al.*, reported the detection of acetone using a mid-infrared laser and selected the wavelengths of detection considering interfering molecules, and demonstrated the low-concentration detection of acetone.

In this paper, our study is aimed at evaluating the system performance for minimum detectable concentration and minimum detection range of the system using an OPO (3-0-3.45 μm) laser based differential absorption lidar system. Our study focuses on the design parameters and atmospheric conditions to achieve the desired system performance. In the present work, system design analysis has been done by simulating the DIAL signals, SNR, and minimum detectable concentrations for chemical warfare agents, explosive precursors, and toxic pollutants. Sarin as a nerve chemical warfare agent, TDG as a blister agent, Acetone as an explosive precursor, and methane as a toxic pollutant have been considered for analysis purposes. Section 2 describes the basic components of the typical DIAL system, while section 3 describes the design parameters of the DIAL system, atmosphere condition parameters, and chemical properties considered for analysis purposes. Section 4 describes the various Eqns. used for simulation studies. Analysis has been done for the maximum detectable range and minimum detectable concentration of various chemicals under different atmospheric conditions.

2. SYSTEM DESCRIPTION

Figure 1 shows the block diagram of a typical DIAL system operating in the mid-infrared band. An OPO based laser source is used as a DIAL transmitter. It transmits the laser pulses at selected wavelengths into the atmosphere. The backscattered energy after scattering and absorption from the target toxic chemical cloud is received by an optical telescope and is focussed onto a detector after using an interference filter for removing the radiations outside the wavelength band of interest. The signal from the detector goes to the preamplifier for amplification purposes. The transmitter and receiver channels are made coaxial by changing the laser beam path with a series of reflecting mirrors. Data acquisition acquires the detector output and transforms the analog lidar signal into a digital domain signal. An industrial PC with a PCI-based card may be used for data acquisition purposes¹⁹. It is necessary to do the sequencing of operations and precise control of subsystems in any system²⁰. Therefore, all the interfacing of subsystems, processing, and operational sequencing have been implemented in a master controller. After processing, the results are displayed on a user-friendly GUI. The laser considered in the studies is VIBRANT IR 3034 from M/s OPOTEK, USA

and the detector is an MCT (Mercury Cadmium Telluride) detector (make: VIGO, Poland, model: PVI-2TE-5). The DAQ board is a 12-bit, 30 MSPS PCI bus-based card (PCI1714U) from M/s Advantech.

3. LIDAR EQUATIONS

To perform the analysis of system design, it is necessary to simulate the DIAL return signal for a given set of design parameters. The following set of Eqns.²¹ has been used to estimate lidar return powers for DIAL wavelengths, SNR values, and noise contributions from various sources.

3.1 Equations for Received Lidar Backscattered Power

If a laser pulse of power P_{TR} and duration T with source wavelength of λ_s is transmitted into the atmosphere, the backscattered return power at the input of the detector from a distance D and is given by Eqn. 1.

$$P_R(\lambda_s, D) = P_{TR} \frac{cT}{2} \beta(\lambda_s, D) \xi(\lambda_s) \xi(D) \frac{A}{D^2} e^{-2 \int_0^D \alpha_{at} dt} \quad (1)$$

Where, P_R is the received power onto the detector, c is the velocity of light, $\beta(\lambda_s, D)$ is the volume backscattering coefficient of the atmosphere, $\xi(\lambda_s)$ is the spectral transmission factor of the receiver, $\xi(D)$ is the probability that a return pulse will hit the detector, A is the effective area of the receiver telescope, α is attenuation coefficient of the atmosphere. The coefficient of atmospheric attenuation α , is because of the interaction of laser radiations at a particular wavelength and atmospheric particles i.e., Mie scattering. It depends on the atmospheric conditions, aerosol shape, size, distribution, and concentration. The atmospheric attenuation constant α , can be calculated by the Kim Kruse Model²² as given by Eqn. 2.

$$\alpha = \frac{3.91}{V} * \left(\frac{0.55}{\lambda_s} \right)^{0.585(\sqrt{V})} \quad (2)$$

where, V is the visual range in kilometers and λ_s is the wavelength in microns.

The backscattering coefficient, $\beta(\lambda_s, D)$ is computed from Eqn. 3.

$$\beta = \frac{\alpha}{K} \quad (3)$$

K , depends upon the wavelength of the laser source beam, the size, and the shape of aerosol and atmospheric conditions.

3.2 Equations for DIAL Return Signal from Chemical Cloud

Equation 1 estimates the lidar return power in case of scattering from aerosols only and no chemical is assumed to be present. But, if a chemical cloud is located at distance D_1 with thickness ΔD so that $\Delta D = D_2 - D_1$, then the chemical will absorb some of the energy at transmitted wavelengths. As mentioned earlier, two wavelengths i.e., λ_{on} and λ_{off} are transmitted for the detection of chemicals using DIAL. In this case, the power received at two wavelengths from distances D_1 and D_2 is given by Eqns. 4-7.

Power received P_1 at λ_{on} from D_1

$$P_1(\lambda_{on}, D_1) = P_{TR_{on}} \frac{cT}{2} \beta_{1_{on}}(\lambda_{on}, D_1) \xi_{on}(\lambda_{on}) \xi(D_1) \frac{A}{D_1^2} e^{-2 \int_0^{D_1} \alpha_{on} dt} \quad (4)$$

Power received P_2 at λ_{on} from D_2

$$P_2(\lambda_{on}, D_2) = P_{TR_{on}} \frac{cT}{2} \beta_{2_{on}}(\lambda_{on}, D_2) \xi_{on}(\lambda_{on}) \xi(D_2) \frac{A}{D_2^2} e^{-2 \int_0^{D_2} \alpha_{on} dt} e^{-2 \int_{D_1}^{D_2} \sigma_{on} N_a dt} \quad (5)$$

Power received P_3 at λ_{off} from D_1

$$P_3(\lambda_{off}, D_1) = P_{TR_{off}} \frac{cT}{2} \beta_{1_{off}}(\lambda_{off}, D_1) \xi_{off}(\lambda_{off}) \xi(D_1) \frac{A}{D_1^2} e^{-2 \int_0^{D_1} \alpha_{off} dt} \quad (6)$$

Power received P_4 at λ_{off} from D_2

$$P_4(\lambda_{off}, D_2) = P_{TR_{off}} \frac{cT}{2} \beta_{2_{off}}(\lambda_{off}, D_2) \xi_{off}(\lambda_{off}) \xi(D_2) \frac{A}{D_2^2} e^{-2 \int_0^{D_2} \alpha_{off} dt} e^{-2 \int_{D_1}^{D_2} \sigma_{off} N_a dt} \quad (7)$$

where, $P_{TR_{on}}$ and $P_{TR_{off}}$ are the laser source transmitted powers for λ_{on} and λ_{off} respectively. N_a is the concentration of the toxic chemical agent averaged over the range of $D_2 - D_1$, σN is the contribution from the absorbing toxic chemical agent; σ_{on} & σ_{off} are the absorption cross-sections of the toxic chemical at online and offline wavelengths respectively. It is assumed that λ_{on} and λ_{off} are so close to each other that they satisfy the following criteria

$$|\lambda_{off} - \lambda_{on}| \leq \frac{|\beta_{off} - \beta_{on}|}{\beta_{on} |K|} \lambda_{on} \quad (8)$$

In the case of a topographic target, the general Eqn. for received power at wavelength λ is given by Eqn. 9.

$$P(\lambda_s, D) = P_{TR} R_T \xi(\lambda_s) \xi(D) \frac{A}{D^2} e^{-2 \int_0^D \alpha_{at} dt} e^{-2 \int_{D_1}^{D_2} N_a dt} \quad (9)$$

where, R_T is the reflectivity of the topographic target.

For Mie scattering, the value of K varies between 1.2 and 2.5. if we assume that $\alpha_{on} \approx \alpha_{off}$ then the Eqns. (4) to (9) can be simplified and N_a can be calculated as

$$N_a = \frac{1}{2(\Delta\sigma)(\Delta D)} \left\{ \ln \frac{P_1}{P_3} + \ln \frac{P_4}{P_2} + \ln \frac{\beta_{1_{off}} \beta_{2_{on}}}{\beta_{1_{on}} \beta_{2_{off}}} \right\} \quad (10)$$

3.3 Signal to Noise Ratio

Noise plays a prominent role in the receiver channel performance of the system. The signal can be detected only if it is above some Signal to Noise Ratio (SNR) baseline. SNR depends on many factors including detection distance and thermal background conditions. The effects of background radiation, detector noises such as dark noise and Johnson noise, and the effect of atmospheric interfering molecules add to the noise contributions in the lidar signal. The contributions of both solar and terrestrial heat radiation are very minor in the mid-IR region (the range of interest), and may thus be disregarded. The expressions for various noises are given by the following Eqns.

3.3.1 Optical Background Noise Power

The receiving mirror’s background noise power is given by Eqn. 11.

$$P_b = T_\lambda \Delta\lambda \Omega_m A L_\lambda \tag{11}$$

where, T_λ is the atmospheric transmittance at wavelength λ , $\Delta\lambda$ is the optical bandwidth of the detection system (μm), Ω_m is the receiving mirror field of view (Sr), A is the area of the receiver telescope (m^2) and L_λ is the spectral radiance ($\text{Wm}^{-2}\mu\text{m}^{-1}\text{sr}^{-1}$) of background source at wavelength λ .

3.3.2 Johnson Noise

Johnson noise power contribution from the detectors is given by Eqn. 12

$$P_j = \frac{4kTB}{R_{sh}} R_L \tag{12}$$

where, T is the temperature of the detector, B is the electrical bandwidth, k is Boltzmann’s constant, R_{sh} is the shunt resistance and R_L is the load resistance of the detector. It is found that the value of Johnson noise is in the order of 10^{-14} watts.

3.3.3 Dark Current and Shot Noise

The dark current is the leakage current produced by the detector when no radiation is falling on its surface. Shot noise power caused by the dark current of the detector is given below by Eqn. 13.

$$P_s = (2q_i B) R_L \tag{13}$$

where, q is the charge, i_d is the dark current, R_L is the load resistance and B is the electrical bandwidth. Under given conditions, this value is found to be in the order of 10^{-20} watts.

3.3.4 Contribution of Interfering Molecules

Some atmospheric trace gases are normally present in the atmosphere. The presence of these interfering molecules affects the atmospheric transmission properties of the laser as these molecules absorb the laser radiations. The most prevalent radiation absorbers in the wavelength band under consideration are CO_2 , C_2H_2 , C_2H_4 , C_2H_6 , NH_3 , NO_2 , O_3 , CH_4 , and H_2O^{23} . These molecules are present in ppb levels to ppm levels of concentration. Typical concentrations of these trace gases in the urban atmosphere are 50 ppb for ammonia, ethylene, ozone, and 6000 ppm for water vapor. Methane and water vapor make up the majority of interfering effects. The concentration of atmospheric methane is normally 2 ppm, while the concentration of water vapors varies with geographic locations and weather cycles.

Although, the ambient concentration of water vapors is high, their absorption is 1 to 2 orders lesser than that of toxic chemicals considered. The absorption cross-section of water vapors in all these lines is of the order of 10^{-27} to 10^{-29} m^2 . Therefore, it does not introduce much error in the actual signal. The data on the error budgeting on the selected wavelength pairs for considered chemicals have been analyzed at all the wavelengths. The error in signal estimation is less than 3 per cent. For methane lines, the maximum reduction in the signal is expected to be 1.293 per cent for offline wavelength while it is 0.08 per cent for online wavelength for methane. For sarin detection, the errors are 0.251 per cent & 0.075 per cent at online

and offline wavelengths respectively. For acetone detection, this value is 0.32 per cent and 0.13 per cent at online & offline wavelength pairs. For TDG detection errors are 2.98 per cent at online wavelength & 0.77 per cent at offline wavelength.

The detection capability of the system is analysed by analysing the SNR of the DIAL signals.

$$\text{SNR} = \sqrt{n} \frac{P_{TR}}{\text{NEP}} \tag{14}$$

where, P_{TR} is the power received, NEP is the noise equivalent power of the detector and n is the number of received pulses used for integration.

The Noise Equivalent Power (NEP) is defined as the signal power required to obtain a unity signal to noise ratio in the presence of some known (detector or background) noise²⁴.

NEP of a detector is given by:

$$\text{NEP} = \frac{\sqrt{(A_{det} B)}}{D^*} \tag{15}$$

where, D^* is the detectivity of the detector, A_{det} is the area of the detector, and B is the bandwidth of the detector.

4. SYSTEM PARAMETERS USED IN SIMULATION STUDIES

The objective of this simulation work is to study the design aspects to realize a compact and portable multiwavelength Differential Absorption Lidar for chemical detection at standoff distances. Accordingly, all subsystem parameters have been worked out based on the COTS items to meet the requirements. The detailed specifications of the proposed system design are described below. Table 1 illustrates the specifications of the trans-receiver system considered for the present study. In this paper, we have considered chemicals such as Sarin (nerve agent

Table 1. DIAL system parameters

Parameter	Value
Transmitted energy for λ_{on} and λ_{off}	5 mJ
Pulse width	6 ns
Receiver telescope diameter	203 mm
Receiver FOV	1 mrad
Detectivity of detector	1×10^9 m.sqrt (Hz)/W
Detector area	1×1 mm^2
Responsivity	1.3 A/W
Detector bandwidth	10 MHz
Data Acquisition sampling rate	30 MSPS
DAQ resolution	12 bits

Table 2. Spectral data of toxic chemicals

Agent	λ_{on} (nm)	λ_{off} (nm)	Delta sigma (m^2)	Toxicity limits
Sarin	3348	3330	1.191×10^{-23}	18 ppm ²⁵
TDG	3190	3300	7.024×10^{-23}	6610 mg/Kg ²⁶
Methane	3316	3326	5.12×10^{-24}	1000 ppm ^[27]
Acetone	3362	3254	2.799×10^{-24}	1000 ppm ^[28]

Table 3. Atmospheric conditions

Atmospheric condition	RH (%)	Temperature (K)	Visibility (Km)	Attenuation coefficient (α) m^{-1}	Backscattering coefficient β ($m^{-1} sr^{-1}$)
Clear	50	298	20	0.021×10^{-3}	4.18×10^{-5}
Moderately haze	80	298	7	0.061×10^{-3}	8.10×10^{-6}
Haze	90	298	3	0.324×10^{-3}	1.52×10^{-6}

category), TDG (blister agents), Acetone (explosive precursor) & Methane (hazardous chemical).

Accordingly, we have considered one chemical for each category for analysis purposes. Table 2 presents the spectral characteristics of these hazardous chemicals²⁵⁻²⁸. We have extended our design analysis to evaluate detection performance under various weather conditions. Table 3 describes the atmospheric conditions under which the system has to perform.

5. RESULTS & DISCUSSION

Using the Eqn.s given in the previous section, the backscattered signal has been simulated for both online and offline wavelengths for DIAL detection. As an example, Fig. 2 shows the DIAL optical signal after transmitting one laser pulse in the open atmosphere each at λ_{on} (online wavelength: 3190 nm) & λ_{off} (offline wavelength: 3300 nm) for TDG. A clear atmospheric condition and no chemical (TDG) is considered to be present in the atmosphere. The figure also shows the Noise Equivalent power (NEP) and SNR baseline which is taken as 10 for the faithful signal detection.

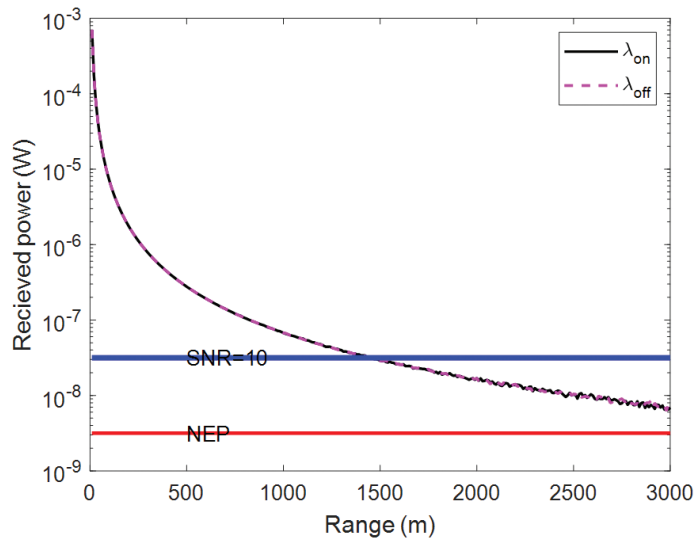


Figure 2. Lidar signal in range resolved conditions and when no chemical present.

It is seen from Fig. 2 that the lidar signal is exponentially decaying with respect to range and eventually crosses the SNR baseline after a particular range. This poses a limit to the range for the detection of chemicals using the system. This is 1470 m in the present case.

In general, chemical agents are released in the atmosphere through artillery shells or UAVs, whereas hand grenades are used to release chemical agents on the ground. Hand grenades normally release 100 s of ppm (concentration) of chemical at the time of detonation depending on the container size of hand

grenades and chemicals used, etc. In our calculations, we have assumed a grenade that releases 200 ppm of concentration at the initial stage. Laser radiations have been transmitted parallel to the ground about 5 m above the surface towards the chemical release location. The chemical release has been considered at 400 m from the system location. Backscattered radiations at two wavelengths have been simulated under clear weather conditions. Aerosol scattering and chemical absorption signals only have been considered in the calculations. All input

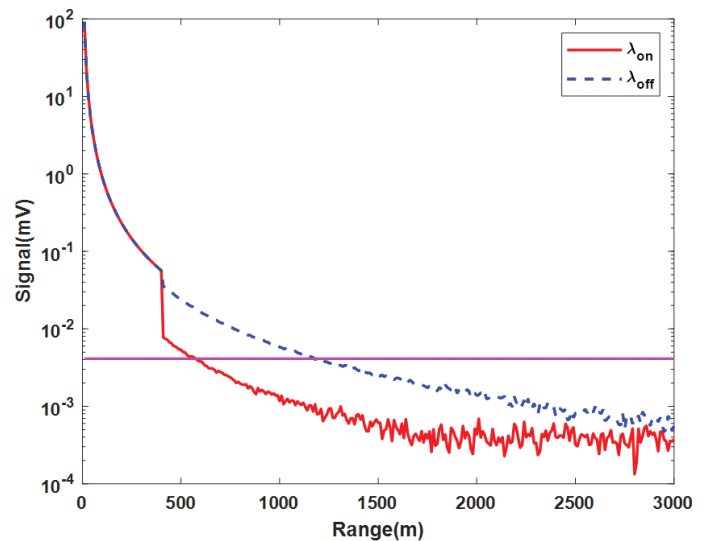


Figure 3. Lidar signal in range resolved conditions and when TDG present.

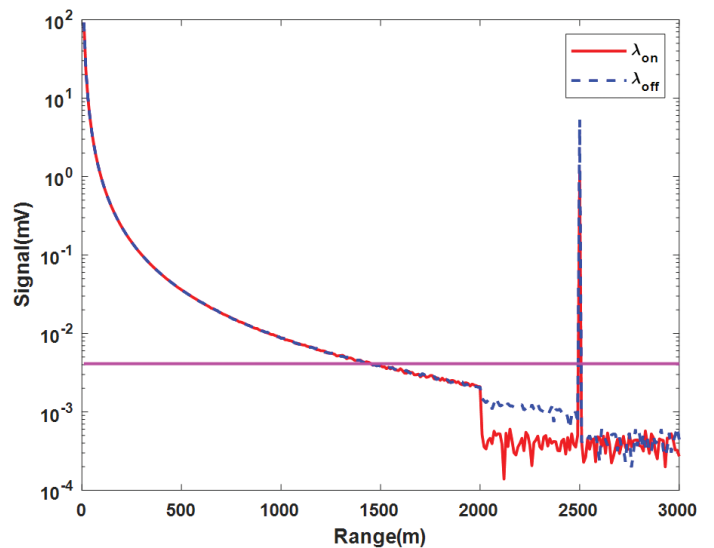


Figure 4. Lidar signal from TDG cloud of 200 ppm concentration located at 2 km in the presence of cooperative target at 2.5 km.

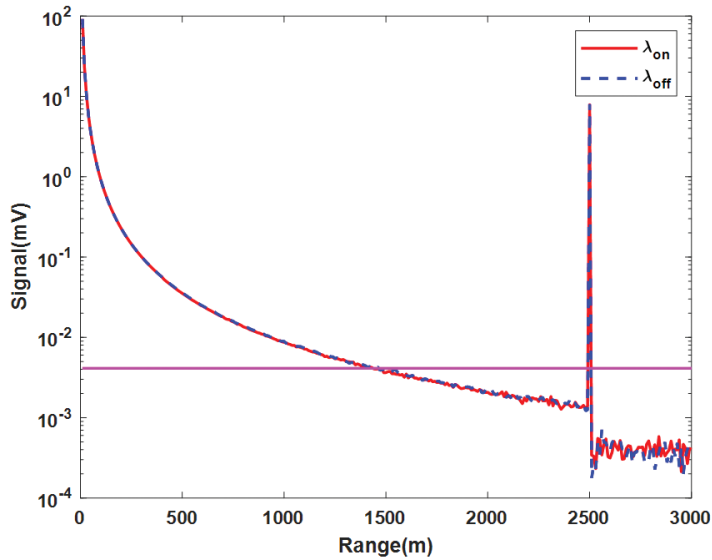


Figure 5. Lidar signal for detection of 2 ppm of TDG in the presence of topographic target.

parameters have been taken from Table 1, Table 2, and Table 3. The optical power and NEP are mapped into the corresponding electrical signal using detector parameters. The results are shown in Fig. 3. It is seen from the results the maximum detectable range for the detection of 200 ppm concentration is reduced to 580 m limiting the capability of the system to detect high concentrations in range resolved or free space measurements.

Now, if a topographic target is introduced at 2500 m, then the signal will be enhanced above SNR due to the reflectivity of the target. A reflectivity of 0.1 is considered for present studies as most of the common topographic targets such as vegetation trees, rocks, etc. have a reflectivity of this order²⁹⁻³⁰. Figure 4 shows the signals at DIAL wavelengths of TDG with the presence of 200 ppm of concentration of TDG. It is seen that now an enhanced signal is available at 2.5 km to detect chemicals. The signals are above the SNR values and the detector can sense the optical power and can discriminate from noise. The signal differential also plays a critical role in deciding the system detection capability in terms

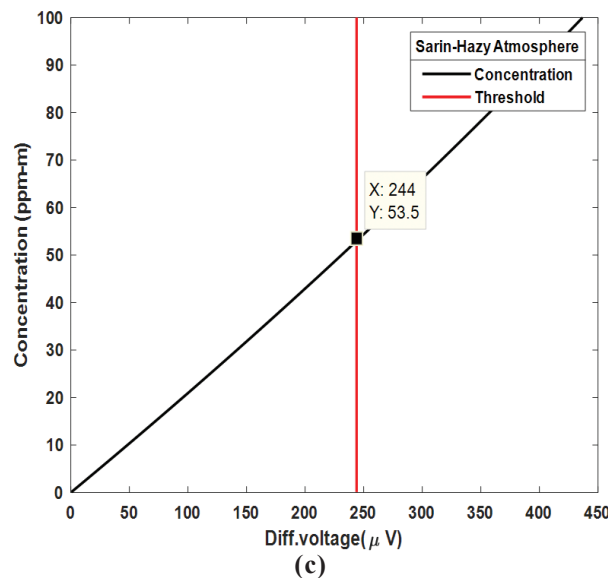
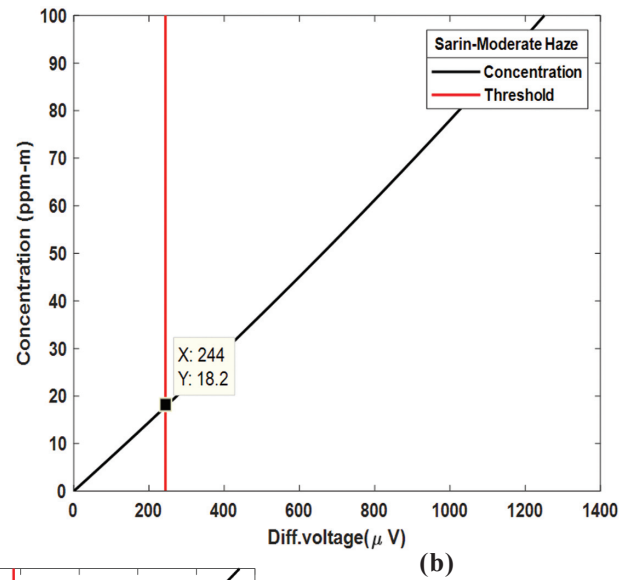
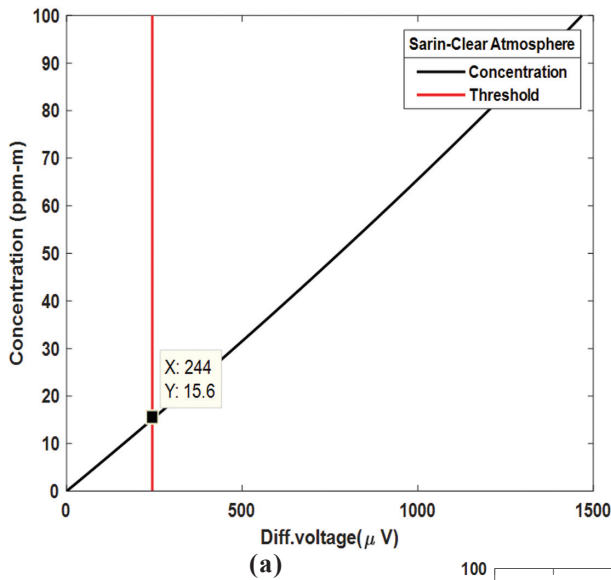


Figure 6. Minimum detectable concentration of sarin under different atmospheric conditions (a) Clear atmosphere, (b) Moderately hazy atmosphere, and (c) Hazy atmosphere.

of the voltage resolution capability of the digitiser. As per the digitizer considered and based on the availability, it is $244 \mu\text{V}$. The online and offline signals shown in Fig. 4 has a differential voltage of 4.15 mV which is much above the threshold value. So, a concentration of 200 ppm of TDG released at 2000 m can be detected in the presence of a topographic target at 2500 m .

Once the chemical is released from the rocket shell or grenade in open atmospheric conditions, the concentration is very high at the time of release, but the chemical disperses with wind and its concentration goes on decreasing with time. The presence of a low concentration of the chemical produces a low differential signal at DIAL wavelengths. This in turn puts a limitation on the system's capacity to detect low levels of concentration of chemicals. Figure 6 shows the DIAL detection of 2 ppm of TDG released at 400 m and a topographic target at 2500 m . The signal differential is $121 \mu\text{V}$ which is below the detection threshold of electronics. So, the system is not

capable of detecting 2 ppm concentration. We analyse that with increasing concentration, the differential in voltage increases; and at a particular concentration, the differential cross the threshold. That value of concentration is considered to be the minimum detectable concentration capability of the designed system. In the present case, it is 3.5 ppm for TDG.

The atmospheric conditions also impact severely the atmosphere transmission properties of the laser. With changing atmospheric conditions, the attenuation coefficient and backscattering vary significantly, thereby affecting the DIAL system performance. As a result, the minimum detectable concentration of a particular chemical by the system is different for different atmospheric conditions. Figure 5 shows the plot of differential voltage at two DIAL wavelengths vs concentration path length for a topographic target at 2000 m at different atmospheric conditions i.e., clear, moderate haze conditions and hazy

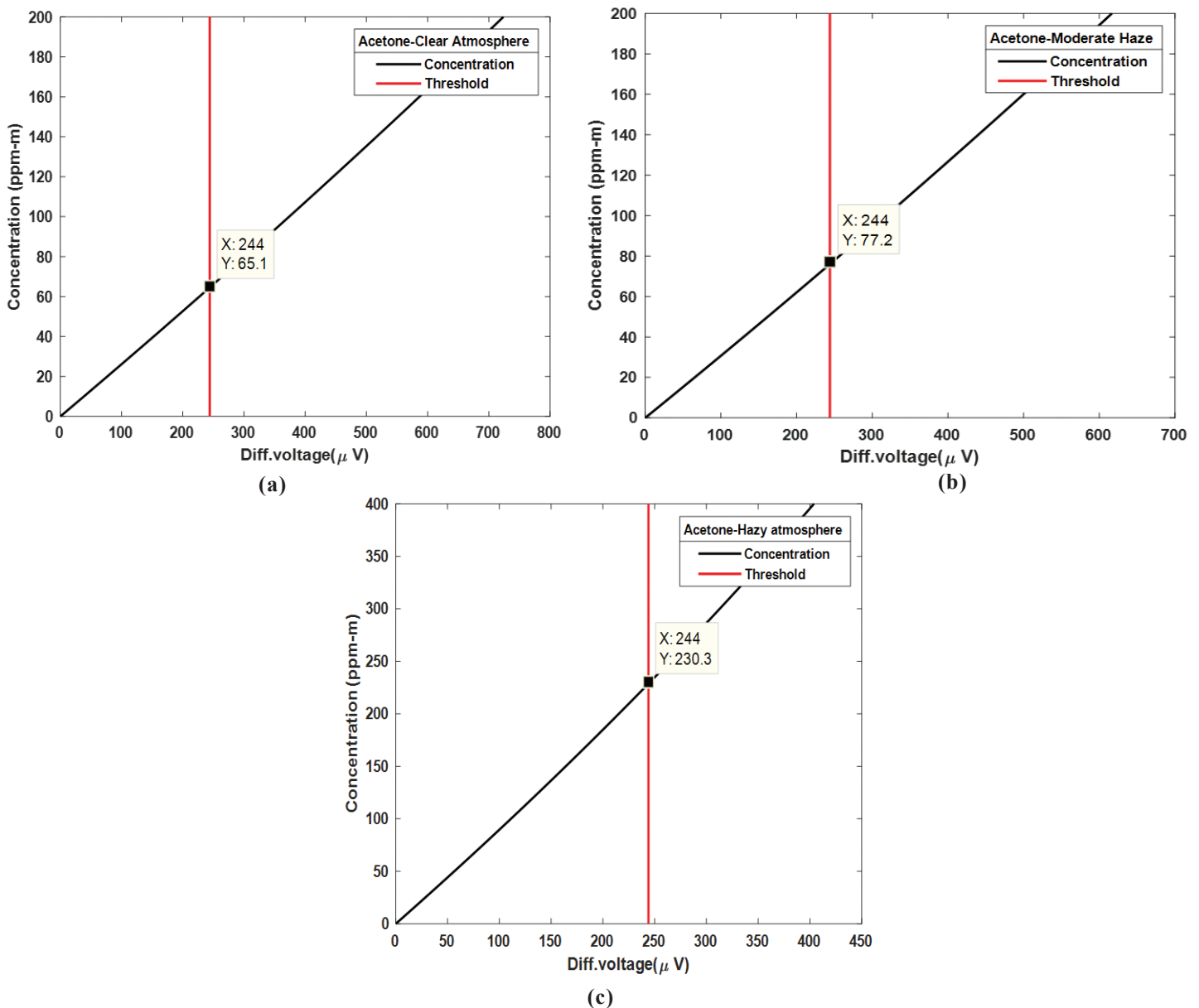


Figure 7. Minimum detectable concentration of acetone under different atmospheric conditions: (a) Clear atmosphere, (b) Moderately hazy atmosphere, and (c) Hazy atmosphere.

Table 4. Minimum detectable concentration of different chemicals under various weather conditions for topographic target present at 2 km

Toxic chemical	λ_{on} (nm)	λ_{off} (nm)	Delta sigma (m ²)	Minimum path length concentration (ppm-m)		
				Clear	Moderate haze	Haze
Sarin	3348	3330	1.191×10^{-23}	15.6	18.2	53.5
TDG	3190	3300	7.024×10^{-23}	3.2	3.8	9.2
Methane	3316	3326	5.12×10^{-24}	41.0	49.4	-
Acetone	3362	3254	2.799×10^{-24}	65.1	77.2	230.3

atmospheric conditions. Different levels of concentrations of Sarin chemical warfare agent have been introduced at 500 m. It is seen that the minimum detectable concentration of Sarin is 15.6 ppm.m and is lowest in clear atmospheric conditions; while the system performance goes down drastically with the minimum detectable concentration going to 53.5 ppm.m under hazy atmospheric conditions.

The second case study is done by analysing the system performance with respect to the minimum detection capability of the system for the detection of Acetone, an explosive precursor and hazardous chemical. Figure 7 shows the differential voltage vs different concentration values of acetone for three different atmospheric conditions. Analysis shows a similar behaviour as the minimum detectable concentration of acetone is three times higher in hazy conditions as compared to clear atmospheric conditions.

Similar calculations have been done for TDG and methane and results are summarised in Table 4.

6. CONCLUSION

Design aspects of the development of a compact and portable OPO laser-based DIAL system have been worked out. This system comprises a tuneable laser operating in 3000-3450 nm wavelength as transmitter and a Cassegrain telescope of 203 mm diameter integrated with TE cooled MCT detector as receiver module, 12-bit, 30 MSPS analog to digital board, etc. Theoretically evaluated the detection capability of Mid Infrared DIAL system for given design specifications under different weather conditions. Performance evaluation was carried out using system parameters to detect toxic chemicals with varying concentrations up to a distance of 2 km. It is concluded that the IR DIAL system with considered design specifications is capable of detecting toxic chemicals in ppm level of concentration up to 2 km with cooperative target conditions. Analysis has been carried out for four types of chemicals with varying concentrations under different weather conditions. It is reported that this system can measure a minimum path-integrated concentration of about 3.2 ppm.m (TDG), 15.6 ppm.m (Sarin), 41 ppm.m (CH₄) & 65.1 ppm.m (Acetone) up to a distance of 2 km under clear weather conditions.

REFERENCES

- Narlagiri, L.M.; Bharati, M.S.S.; Beeram, R.; Banerjee, D. & Soma, V.R. Recent trends in laser-based standoff

- detection of hazardous molecules. *TrAC Trends in Analyt. Chem.*, 2022, 116645. doi: 10.1016/j.trac.2022.116645.
- Jindal, M.K.; Mainuddin, M.; Veerabuthiran, S. & Razdan, A.K. Laser-based systems for standoff detection of CWA: A short review. *IEEE Sensors J.*, 2020, **21**(4), 4085-4096. doi:10.1109/JSEN.2020.3030672.
- Hoffland, L.D.; Piffath, R.J. & Bouck, J.B. Spectral signatures of chemical agents and simulants. *Opt. Eng.*, 1985, **24**(6), 982-984. doi: 10.1117/12.7973613.
- Degtiarev, E.V.; Geiger, A.R. & Richmond, R.D. Compact dual wavelength 3.30 to 3.47-um DIAL lidar. *In Chemical and Biological Sensing*, July 2000. 4036, pp. 229-235. SPIE. doi:10.1117/12.394068.
- Prasad, C.R.; Kabro, P.; & Mathur, S.L. Tunable IR differential absorption lidar for remote sensing of chemicals. *In Application of Lidar to Current Atmospheric Topics III*, 1999, October, 3757. pp. 87-95, SPIE. doi: 10.1117/12.366422
- Robinson, R.; Gardiner, T.; Innocenti, F.; Woods, P. & Coleman, M. Infrared differential absorption Lidar (DIAL) measurements of hydrocarbon emissions. *J. Environ. Monit.*, 2011, **13**(8), 2213-2220. doi:10.1039/c0em00312c.
- Innocenti, F.; Robinson, R.; Gardiner, T.; Finlayson, A. & Connor, A. Differential absorption lidar (DIAL) measurements of landfill methane emissions. *Remote Sensing*, 2017, **9**(9), 953. doi:10.3390/rs9090953.
- Rossi, R.; Di Giovanni, D.; Malizia, A. & Gaudio, P. Measurements of vehicle pollutants in a high-traffic urban area by a multiwavelength dial approach: Correlation between two different motor vehicle pollutants. *Atmosphere*, 2020, **11**(4), 383. doi :10.3390/atmos11040383.
- Boreysho, A.S.; Konyaev, M.A.E.; Morozov, A.V.; Pikulik, A.V.; Savin, A.V.E.; Trilis, A.V.E. & Rozhnov, A.V. Mobile multiwave lidar complexes. *Quantum Electron.*, 2005, **35**(12), 1167. doi: 10.1070/QE2005v035n12ABEH008962.
- Kariminezhad, H.; Parvin, P.; Borna, F. & Bavali, A. SF₆ leak detection of high-voltage installations using TEA-CO₂ laser-based DIAL. *Optics. Lasers Eng.*, 2010, **48**(4),

- 491-499.
doi:10.1016/j.optlaseng.2009.08.011.
11. Simko, M. & Valovsky, M. Field trials of DIAL stand-off detection using CO₂ tunable laser, *In Electro-Optical Remote Sensing XVI*, 2022. 12272, pp. 117-123. SPIE.
doi: 10.1117/12.2636435.
 12. Puiu, A.; Fiorani, L.; Rosa, O.; Borelli, R.; Pistilli, M. & Palucci, A. Lidar/DIAL detection of acetone at 3.3 μm by a tunable OPO laser system. *Laser Physics*, 2014, **24**(8), 085606.
doi: 10.1088/1054-660X/24/8/085606.
 13. Mitev, V.; Babichenko, S.; Bennès, J.; Borelli, R.; Dolfi-Bouteyre, A.; Fiorani, L.; Hespel, L.; Huet, T.; Palucci, A.; Pistilli, M.; Puiu, A. & Sobolev, I. Mid-IR DIAL for high-resolution mapping of explosive precursors. *In Lidar Technologies, Techniques, and Measurements for Atmospheric Remote Sensing IX*, 2013, October, 8894, pp. 140-152. SPIE.
doi: 10.1117/12.2028374.
 14. Romanovskii, O.A.; Sadovnikov, S.A.; Kharchenko, O.V. & Yakovlev, S.V. Development of Near/Mid IR differential absorption OPO lidar system for sensing of atmospheric gases, *Opt. Laser Technol.*, 2019, 116, 43-47.
doi :10.1016/j.optlastec.2019.03.011.
 15. Yakovlev, S.V.; Romanovskii, O.A.; Sadovnikov, S.A.; Tuzhilkin, D.A.; Nevzorov, A.A., Kharchenko, O.V. & Kravtsova, N.S. Mobile mid-infrared differential absorption lidar for methane monitoring in the atmosphere: Calibration and first in situ tests. *Results in Optics*, 2022, **8**, 100233.
doi: 10.1016/j.rio.2022.100233.
 16. Bril, A.I.; Ivanov, A.P.; Kabashnikov, V.P.; Kuzmina, N.V.; Popov, V.M. & Chaikovskiy, A.P. Effects of uncertainties in atmospheric conditions on the accuracy of concentration measurements by the differential absorption method in the 9-to 11-μm and 4.6-to 5.6-μm spectral ranges. *In Sixth International Symposium on Atmospheric and Ocean Optics*, SPIE 1999, 3983, pp. 306-314.
doi: 10.1117/12.370508.
 17. Payne, D.; Schroeder, J. & Liang, P. The importance of accurate atmospheric modelling. *In Remote Sensing of the Atmosphere, Clouds, and Precipitation V*, SPIE, 2014, 9259, pp. 227-242.
doi:10.1117/12.2073519.
 18. Puiu, A.; Fiorani, L.; Rosa, O.; Borelli, R.; Pistilli, M. & Palucci, A. Lidar/DIAL detection of acetone at 3.3 μm by a tunable OPO laser system. *Laser Physics*, 2014, **24**(8), 085606.
doi: 10.1088/1054-660X/24/8/085606.
 19. Mainuddin M.; Beg, M. T.; Tyagi, R.K.; Rajesh, R.; Singhal, G. & Dawar, A.L. Optical spectroscopic based in-line iodine flow measurement system—an application to COIL. *Sensors and Actuators B: Chemical*, 2005, **109**(2), 375-380.
doi: 10.1016/j.snb.2005.01.004.
 20. Cheng, L.; Xie, C.; Zhao, M.; Li, L.; Yang, H.; Fang, Z.; Chen, J.; Dong, L. & Wang, Y. Design of lidar data acquisition and control system in high repetition rate and photon-counting mode: Providing testing for space-borne lidar. *Sensors*, 2022, **22**(10), 3706.
doi: 10.3390/s22103706.
 21. Measures, R.M. *Laser remote sensing: Fundamentals and applications*. New York, Wiley-Interscience, 1984. 521 p.
doi: 10.1029/eo066i040p00686-05.
 22. Kruse, P.W.; McGlauchlin, L.D. & McQuistan, R.B. *Elements of infrared technology: Generation, transmission and detection*. New York: Wiley, 1962.
doi: 10.1016/0038-1101(62)90120-x.
 23. Veerabuthiran, S.; Razdan, A.K. & Sharma, Y. Open path measurement of atmospheric transmission spectra in the region of 3000–3450 nm using tunable mid infrared lidar. *J. Appl. Spectrosc.*, 2020, **86**(6), 1100-1105.
doi:10.1007/s10812-020-00946-y.
 24. Benford, D.J.; Hunter, T.R. & Phillips, T.G. Noise equivalent power of background limited thermal detectors at submillimeter wavelengths. *Int. J. Infrared Millimeter Waves*, **19**, 931-938.
doi: 10.1023/A:1022671223858.
 25. Sayago, I.; Matatagui, D.; Fernández, M.J.; Fontecha, J.L.; Jurewicz, I.; Garriga, R. & Muñoz, E. Graphene oxide as sensitive layer in Love-wave surface acoustic wave sensors for the detection of chemical warfare agent simulants. *Talanta*, 2016, **148**, 393-400.
doi: 10.1016/j.talanta.2015.10.069.
 26. Smyth, Jr., H.F.; Seaton, J. & Fischer, L. The single dose toxicity of some glycols and derivatives. *J. Ind. Hyg. Toxicol.*, 1941, **23**(6), 259-268.
 27. Prasad, S.; Zhao, L. & Gomes, J. Methane and natural gas exposure limits. *Epidemiology*, 2011, **22**(1), S251.
doi: 10.1097/01.ede.0000392463.93990.1e.
 28. Young, J.A. Acetone. *J. Chem. Educ.*, 2001, **78**(9), 1175.
doi: 10.1021/ed078p1175.
 29. Fabre, S.; Lesaignoux, A.; Olioso, A. & Briottet, X. Influence of water content on spectral reflectance of leaves in the 3–15 μm domain. *IEEE Geosci. Remote Sensing Lett.*, 2010, **8**(1), 143-147.
doi: 10.1109/LGRS.2010.2053518.
 30. Salisbury, J.W. & D'Aria, D.M. Emissivity of terrestrial materials in the 3–5 μm atmospheric window. *Remote Sensing Environ.*, 1994, **47**(3), 345-361.
doi: 10.1016/0034-4257(94)90102-3.

ACKNOWLEDGMENT

The authors wish to thank Director, Instruments Research & Development Establishment (IRDE) for his constant support and encouragement in executing the current research work.

This work is supported by the Ministry of Electronics and Information Technology, Government of India under the Visvesvaraya PhD scheme.

CONTRIBUTORS

Mr Mukesh Kumar Jindal obtained his MTech Degree in Process Control from University of Delhi, India. Currently, he is working as Scientist-F in DRDO-IRDE, Dehradun, India. His areas of interest include: Develop control electronics and

software for LIDAR systems like Mie LIDAR, differential absorption LIDAR and Raman LIDAR, etc.

In the current study, he developed the simulation software for carrying out the numerical simulations, carried out the analysis part and contributed in manuscript preparation.

Dr Prof Mainuddin obtained his PhD in 2008 from Jamia Millia Islamia, New Delhi. He is presently working as a Professor at the Department of Electronics and Communication Engineering, Jamia Millia Islamia, New Delhi. His research interests include: Antenna design, laser spectroscopy, optoelectronics, optical diagnostics, sensors and instrumentation and high power lasers, data communication, optical communication and computer networks etc.

For the current study, he supervised the research work and contributed to the final version of manuscript.

Dr S. Veerabuthiran obtained his PhD in the area of 'LIDAR for measurement of atmospheric aerosols and clouds' from Space Physics Laboratory/ISRO. He is working as Scientist F at DRDO-CHESS, Hyderabad. His areas of research interest include: Laser spectroscopy based sensors, development of lidar systems and high power laser based systems.

For the current paper, he developed the theoretical formulation, performed the analysis work and supervised the research work.

Mr Atul Kumar obtained his BTech Degree from Institute of Engineering and Technology, Uttar Pradesh Technical University, Lucknow. He is working as Scientist 'E' in DRDO-IRDE, Dehradun. His area of interests are: Analog design and embedded systems. He has worked on various opto-electronics, software for high power laser and spectroscopy projects. Currently, he is working on the development of lidar systems for clouds and aerosols.

For the current paper, he has contributed in the manuscript writing and analysis of the noise contributions in lidar signal.